EasyChair Preprint

№ 5787

Solar Light Driven Ultra-Fast Photodegradation of RhB Dye by Perovskite/G-C3N4 Nano-Composite

Lopamudra Mohanty and Suresh Dash

June 14, 2021

DR B R AMBEDKAR NATIONAL INSTITUTE OF TECHNOLOGY JALANDHAR-144011, INDIA
International Conference on Recent Development on Materials, Reliability, Safety and Environmental Issues (IMRSE– 2021)

Solar light driven Ultra-fast Photodegradation of RhB dye by Perovskite/g-C_3N_4 nano-composite

Lopamudra Mohanty [1*], Suresh Kumar Dash [2]
Department of Chemistry , ITER, Siksha 'O' Anusandhan (Deemed to be University) ,
Bhubaneswar, Odisha, India, 751030

email: lmohanty1995@gmail.com

Abstract- The recalcitrant and ubiquitous nature of toxic dyes in surface water urgently needs to be treated for decreasing hazardous effects and mitigating water scarcity for sustainability. The composites $BiFeO_3$/g-C_3N_4 and $BiTiO_3$/g-C_3N_4 prepared by sonication have shown higher photo-catalytic degradation of RhB dye by varying parameters such as initial concentration, pH of solution, agitation time and catalyst dose under solar light as compared to g-C_3N_4. The X-ray diffraction pattern showed retention of g-C_3N_4 structure after modification. The Fourier Transform IR spectra showed efficient attachment of perovskite with g-C_3N_4. The $BiFeO_3$/g-C_3N_4 and $BiTiO_3$/g-C_3N_4 composites exhibited highest photo-degradation of 99. % for RhB dye in a short span of 35min., 20 min at pH~3 than the pristine $BiFeO_3$ and $BiTiO_3$/g-C_3N_4 . The kinetics of the photocatalytic degradation for RhB followed a pseudo-first order rate for varying concentration and dose. Both $BiFeO_3$/g-C_3N_4 and $BiTiO_3$/g-C_3N_4 are prominent catalysts for ultra-fast degradation of toxic dyes by using solar radiation.

Keywords- perovskite-g-C_3N_4, toxic dye, photodegradation, mechanism, solar light

*Lopamudra Mohanty

1. INTRODUCTION

Water being the matrix of life for living beings has to be pure, portable and abundant. Due to population growth and rapid urbanisation the scarcity and contamination of water has become alarming. According to UN World Water Development Report 2020, such a deterioration of the situation would only hinder achievement of Sustainable Development Goal 6 which is part of the 2030 Agenda for Sustainable Development [1,2]. Amongst various contaminants, the industrial effluents containing organic dyes are extremely toxic causing vomiting, nausea, and endocrine disruption even at meagre concentrations leading to human health menace. The textile, leather tanning and finishing industrial effluents contain 10–15% of organic dyes that are carcinogenic and mutagenic on human beings and destroy aesthetic and environmental values. The ubiquitous nature and complex structure of dyes make it difficult for de-colourisation and complete mineralization for its degradation. Among various methods, the use of photocatalytic degradation with eco-friendly photocatalysts is considered a more potential approach. Recently, much work has been carried out to develop new cost effective, environmentally benign and easy to prepare fascinating materials for photo-catalytic degradation of dyes[3].

Rhodamine B (RhB: $C_{28}H_{31}ClN_2O_3$) dye is highly unfavourable to the aquatic ecosystem and pose threat to the animals and human beings. The adsorptive removal of dyes by $Bi_7O_9I_3$-$MgAl_2O_4$ and Mg doped cobalt ferrite spinel nanoparticles have been well documented[4]Visible light driven Azo dye degradation by $CoTiO_3$ and magnetic $MgFe_2O_4$-$MgTiO_3$ perovskite nano composites were also reported[5,6]. In recent years, a novel non-metallic polymeric semiconductor, g-C_3N_4 has received greater importance in various visible light photocatalytic applications because of its exceptional chemical stability, environmental acceptance, low-cost,

non-toxicity and tunable band gap. However, bulk g-C_3N_4 exhibits short lifetime and easy recombination and decreased quantum efficiency because of its small surface area and fast recombination rate of photogenerated charge carriers[7]. Much effort has been made to solve the disadvantages of g-C_3N_4, including porous structure construction, metal or non-metal elements doping, and other semiconductors coupling. The composites of g-C_3N_4 have established more efficacy by enhancing the photocatalytic performances by tunable band gap and decreasing electron/hole recombination. The valence band level in the modified system is shifted to more positive value enhancing the oxidation ability. The examples include g-C_3N_4/Ag_3PO_4, $Cd_{0.5}Zn_{0.5}S$/g-C_3N_4, and $CoTiO_3$/g-C_3N_4. Much work has been carried out for photo degradation of toxic dyes under visible light by layer-type perovskite synthesized by ion exchange method [8,9]. In the present study, excellent degradation of a fluorescent dye Rhodamine B was achieved in a short period of 20 min and 35min. by making a composite of g-C_3N_4 with $BiTiO_3$ and $BiFeO_3$ under solar light.

2. MATERIALS AND METHODS

2.1 Materials

All the chemicals were of analytical grade. Melamine, $Bi(NO_3)_3.9H_2O$, NH_4VO_3, Sodium hydroxide (NaOH), , Rhodamine B etc. were used without further purification.

Synthesis of g-C_3N_4

Graphitic carbon nitride (g-C_3N_4) was synthesized by using simple pyrolysis method. An amount of 6 gm of melamine was placed in to an alumina crucible with lid and heated at 550 °C for 4 h with a heating rate of 10 °Cmin^{-1}. After 4 hr it cooled down naturally and then it was ground to form powder[10].

Synthesis of $BiFeO_3$

$Bi(NO_3)_3.9H_2O$ and $Fe(NO_3)_3.9H_2O$ were dissolved in Required amount of acetic acid and water to form a transparent solution. Then required amount of citric acid was added to the above solution. The solution was stirred for 1hr and then it was evaporated at 70°C for 2hr.Then the solution was centrifuged and washed several times with distilled water until the pH of the solution was neutral. Then the precipitate was oven dried at 70°C overnight and followed by calcination in a muffle furnace at 500 °C for 4hrs[11]. The obtained sample was named as BFO for further experimentation.

Synthesis of $BiTiO_3$

For the preparation of $BiTiO_3$ required amount of aqueous solution of $Bi(NO_3)_3.9H_2O$ was prepared using distilled water. The required amount of TiO_2 powder was added to the above prepared solution with continuous stirring. The suspension was sonicated for 10 min for the breakdown of TiO_2 agglomerates. Then oxalic acid solution was added to the above solution under continuous stirring at a pH of 6-7 by using ammonia solution. The obtained precipitate was centrifuged and washed with distilled water repeatedly and dried in vacuum oven at 70°C overnight. Finally the precipitate was calcined at 500 °C for 4hrs[12] The obtained sample was named as BTO for further experimentation.

Synthesis of $BiFeO_3$/ g-C_3N_4 and $BiTiO_3$/ g-C_3N_4

For the synthesis of $BiFeO_3$/ g-C_3N_4 and $BiTiO_3$/ g-C_3N_4 an amount of 2gm of g-C_3N_4 was taken in 100ml of water and then the solution was sonicated for 15min. The $BiFeO_3$ and $BiTiO_3$ powder were added separately to the above solution and again sonicated for 15min. The whole solution was centrifuged and washed with distilled water and dried in an oven at 70°C for 12 h and calcined at 400 °C for 4hrs[11] .The obtained samples were named as BFO-g-CN and BTO-g-CN for further experimentation.

3.Result discussion

3.1 XRD analysis

Figure 1. shows the powdered X-ray diffraction of the samples observed in the range of 2θ = 10–80°. For BFO, the intense peaks appeared at angles 2θ value of 30.9°, 32.1°, 36.1° corresponded to the planes (110), (113) respectively. For BTO the intense peaks appeared at angles 2θ value of 30°corresponded to the plane(171). The peaks obtained at 2θ values 13.1° and 27.1° referred to the (100) and (002) plane of g-C3N4[12,13].

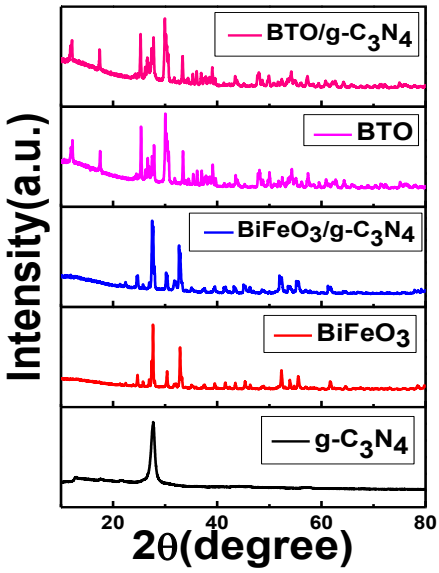

Fig1: Powdered XRD analysis of g-C_3N_4, BFO, BFO -g-CN, BTO and BTO-g-CN.

3.2 FESEM

Figure 2. shows the FESEM images of the samples which shows that the pristine BFO particle has regular sphere like structure with a diameter range of 10 micrometer. When g-CN particle having flake like structure was added to this BFO particle having spherical shape,the morphology of the BFO particle slightly disappears in the composite[14]. Figure3shows the formation process of BFO-g-CN. In case of BTO, the FESEM image shows that it has spherical ans spheroidical shape as shown in fig2(c) and in case of BTO-g-CN the shape remain unchanged i.e there is no deformation of the composite[15].

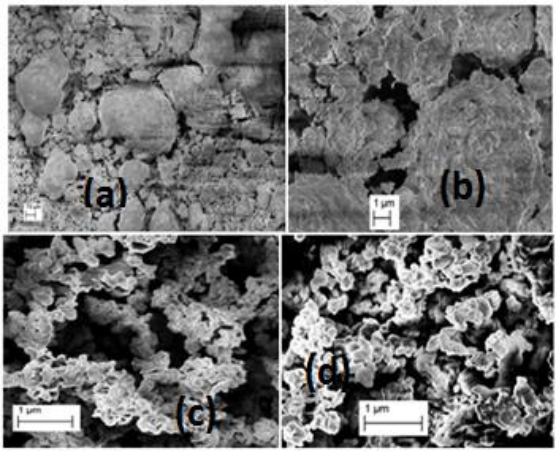

Fig2: FESEM images of (a) BFO(b) BFO -g-CN(c) BTO and (d)BTO-g-CN

3.3 EDAX Analysis

Figure 3. shows the EDAX Analysis of the samples which concludes the perfect preparation of the samples by the presence of required elements in the samples.In BFO(fig.4a) there is the presence of Bi,Fe,O and in BFO-g-CN(fig.4b) there is presence of elements of BFO as well as the presence of C,N for g-CN.Simillarly in BTO (fig.c) there is presence of Bi,Ti,O elements and in BTO-g-CN(fig.4d) there is presence of elements of BFO as well as the presence of C,N for g-CN[16].

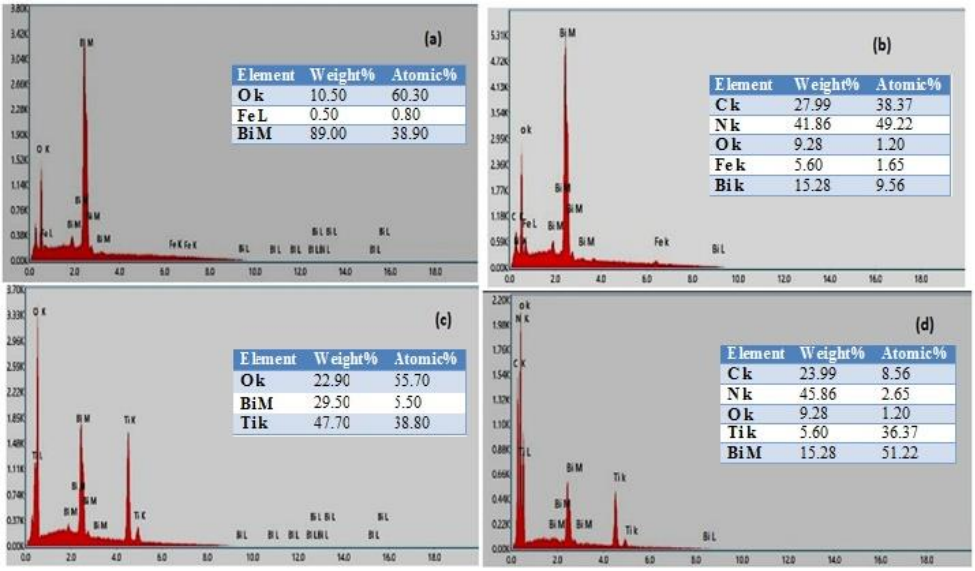

Fig3: EDAX Analysis of (a) BFO(b) BFO -g-CN(c) BTO and (d)BTO-g-CN.

3.4. FTIR

Figure 4. shows the FTIR spectra of the samples. Several strong bands in the1200-1650 cm-1 region indicates the stretching modes of CN heterocycles. Another band 801 cm^{-1} is for the breathing mode of the triazine units. broad band at around 3000 cm^{-1} are indicative of NH stretching vibration modes. The FT-IR spectra of BFO Shows a broad absorption band around 560 cm^{-1} for Fe-O bending vibration . In BTO a sharp peak occurs at 1376 cm^{-1} for N-O stretching vibration,817 cm^{-1} for Ti-O stretching vibration[17].

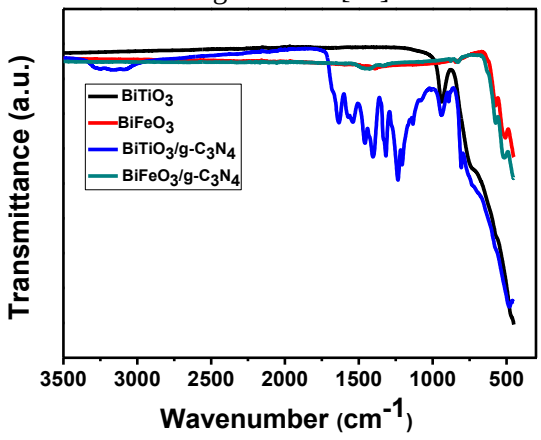

Fig4. FTIR spectra of g-C_3N_4, BFO, BFO -g-CN, BTO and BTO-g-CN

3.5 Photocatalytic performance

The photocatalytic efficiency of BFO, BFO-g-CN,BTO and BTO-g-CN samples were studied by photo degradation of RhB under natural sunlight irradiation with asbestos cover to protect penetration of UV radiation. An amount of 10 mg of the catalyst was dispersed in 25 mL of the dye solution (10 ppm RhB aqueous solution). Before irradiation of light, the solution was stirred

for 30 min in the dark to study the adsorption-desorption equilibrium. At the each time intervals of every 15 min, 2 mL of the sample was withdrawn from the reaction solution and then centrifuged to remove the particles during the photocatalytic degradation. Then the concentration of dyes after degradation were examined by UV–vis spectrophotometer(Systronic PC. Based Double Beam UV-Visible spectrophotometer,2202), at the absorbance wavelength of 553 nm for RhB.

3.5.1 Effect of pH value of the solution

The pH of the solution plays an crucial role in the photo catalytic degradation of dye solution. The rate of reaction and surface charge of g-C_3N_4 varies with the any change in pH solution. Thus the surface of the g-C_3N_4 may be positively or negatively charged according to the value of pH_{zpc} (The zero point charge is responsible for adsorption) when it is in acidic or basic medium. The degradation of RhB occurs in the alkaline medium as both dyes are the cationic dyes so at higher pH, the cations are dissociates easily. In alkaline medium, hydroxyl radical (•OH) an oxidant can be formed, thus increasing the rate of photo degradation of the dye. As showed in the Figure 5., at pH 3 the percentage of degradation is maximum compared to other pH conditions[18].

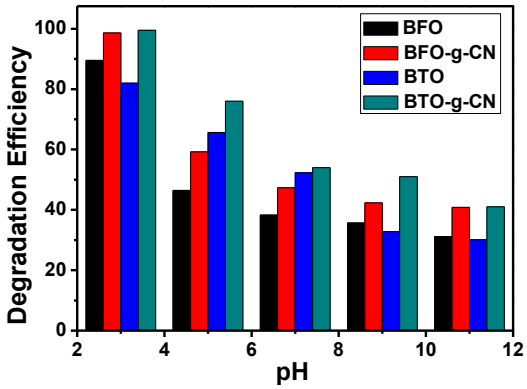

Fig5. pH vs %Degradation of BFO, BFO -g-CN, BTO and BTO-g-CN

3.5.2 Effect of Initial Concentration

The initial concentration of dye solution is an important parameter in determining the adsorbed amount of dye on the surface of catalyst, that controls the photo degradation. The percentage degradation decreases with increase in the concentration of dye, may be attributed to i)With increase in the amount of dye the adsorption reaches an optimum value on the surface of catalyst leading to non-availability of the active sites ii) On increasing the concentration of dye, the number of incident photons on catalyst surface is diminished hence the excitation of photocatalyst is decreased. As shown in Figure 6., the percentage of degradation gradually decreases on increasing the concentration of dye after [19].

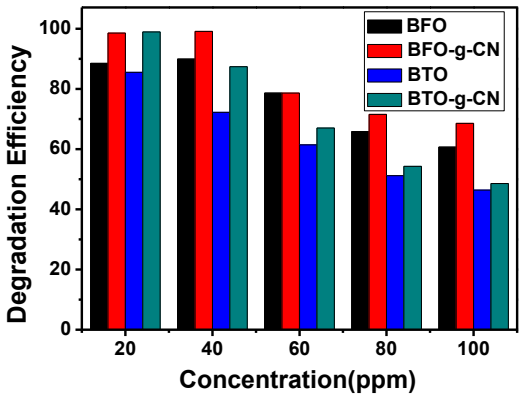

Fig6. Concentration vs %Degradation of BFO, BFO -g-CN, BTO and BTO-g-CN

3.5.3 Effect of adsorbent dose

The degradation of RhB decreased with an increase in dose after 60mg. Due to increase in amount of the substance the remaining sites become difficult to occupy because of the repulsive forces between the solute molecule of the solid and the bulk phases. The uptake capacity of the dye decreased may be due to two factors. Firstly, the increase in the amount of adsorbent developed clumsiness in the number of active sites for optimum adsorption, thus decreasing the uptake of dyes. Secondly, the acidic functional groups that were freely available to RhB, encounter a competition of basic groups from active carbon with increase in their amount as displayed in Figure 7 [20].

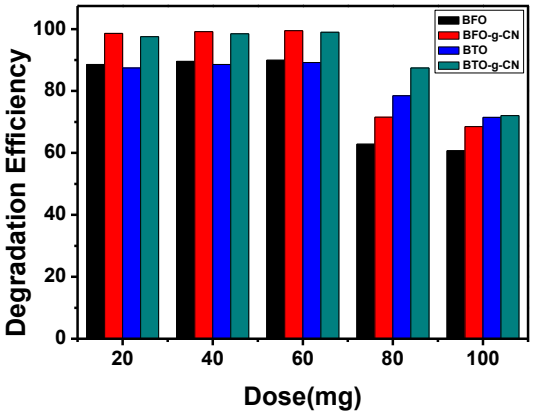

Fig7. Dose vs %Degradation of BFO, BFO -g-CN, BTO and BTO-g-CN

3.5.4 Effect of agitation Time

Fig.8shows the UV-Vis spectra of RhB after different irradiation times in presence of BFO, BFO-g-CN,BTO and BTO-g-CN photocatalysts. The main absorption peak of RhB observed at 554nm .The peak of RhB were disappear within 35min(b).,20min. (d)by BFO-g-CN and BTO-g-CN where as BFO and BTO takes 60min. and 50min. rspectively suggesting the excellent photocatalytic degradation of the BFO-g-CN,BTO and BTO-g-CN photocatalysts than the pristine BFO and BTO.

The percentage of dye degradation increased with increase in agitation time. The crowdedness caused by the bulky dye molecules on the surface hinders the rhythm of adsorption, reaching a state of equilibrium [21].Fig.9 shows that about 99% of RhB was degraded by BFO-g-CN and BTO-g-CN within a certain time limit.

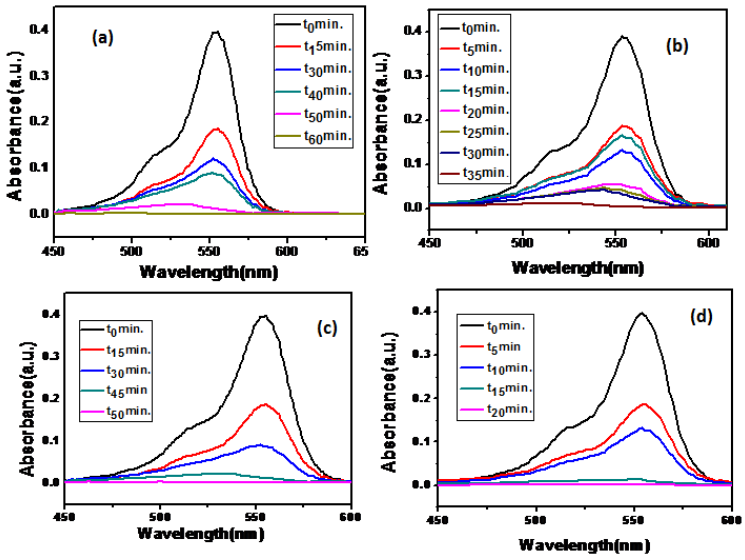

Fig8. UV–Vis spectra of RhB solution in presence of BFO, BFO -g-CN, BTO and BTO-g-CN

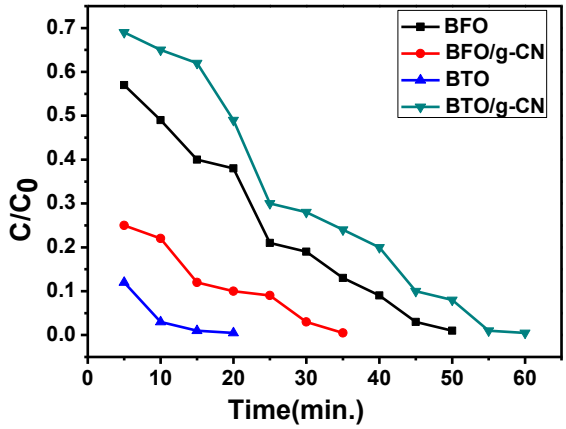

Fig9. C/C_0 versus irradiation time for photodegradation of RhB under visible-light irradiation

4.Kinetic Study

The kinetic data curves and reaction rates, k, for RhB photocatalytic degradation with the samples (BFO-g-CN,BTO-g-CN) are presented in Fig.10. It is clear that the curve with irradiation time as abscissa and $\ln(C/C_0)$ as the vertical ordinate is close to a linear curve, which indicates the photocatalytic degradation of RhB using the samples follows pseudo first-order reaction kinetics. The curves of k for BFO-g-CN,BTO-g-CN are 0.0202 and 0.0101 min^{-1}, respectively, indicating favourable photocatalytic performance of the BFO-g-CNandBTO-g-CN.

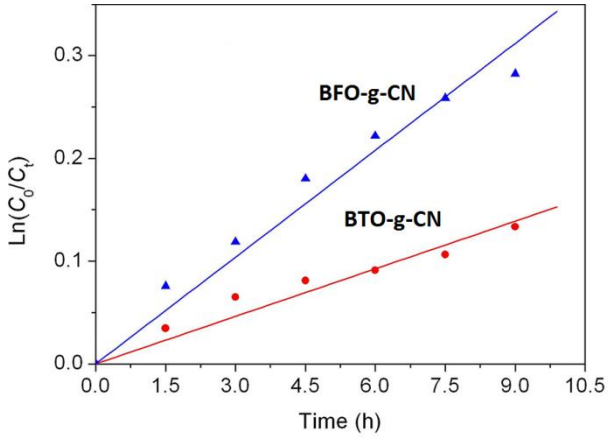

Fig10. Kineticanalysis of BFO -g-CN and BTO-g-CN

Mechanism

Fig.11 Shows the photocatalytic mechanism of BFO-g-CN. When light source falls on the surface of g-C_3N_4, then there will be a generation of photo inducd electron-hole pairs. The CB(-1.22) and VB(1.66) of g-C_3N_4 is more electro negative than CB(0.33) and VB(2.53) potential of $BiFeO_3$. Therefore the photoinduced electron from the CB of g-C_3N_4 can transfer to the CB of $BiFeO_3$. Now this electron reacts with the atmospheric oxygen($O_2^{\cdot-}$) to produce hydroxyl radical(OH^-) which is able to degrade the dyes(RhB and MG) to some stable product. At the sametime the photo inducd holes can transfer from the VB of $BiFeO_3$ to the VB of g-C_3N_4 as the VB potential of $BiFeO_3$ is more positive than the VB potential of g-C_3N_4. Due to this charge transfer process the electron-hole pair recombination will suppress[22]. For BFO-g-CN the mechanism is similar as like as BFO-g-CN.

$$g - C_3N_4/BiFeO_3 + hv \rightarrow e^- + h^+$$

$$e^- + O_2 \rightarrow \bullet O_2^-$$

$$\bullet O_2^- + RhB \rightarrow products$$

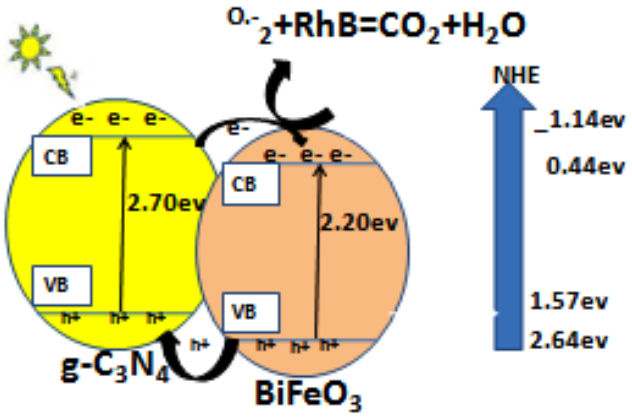

Fig.11 Mechanism of $BiFeO_3$-g-C_3N_4 composite for the Dgradation of RhB under stimulated sunlight.

5.Conclusions

The acute scarcity of pure and safe water has compelled the researchers to opt for ultra-fast and efficient methods for water purification. The recalcitrant and ubiquitous nature of organic dyes in surface water can be easily removed by ternary photo-catalysts BFO-g-CN and BTO-g-CN under solar radiation. The fluorescence Rhodamine B dye was efficiently degraded within a short time interval. The catalyst showed better performance in case of RhB dye which was achieved above 99% degradation within 35min., 20min. Thus the low-cost, easy to synthesize and solar-light responsive catalyst can be highly beneficial for removal of toxic dyes from water.

References

[1] Guppy,L., Anderson,K., 2017. Global water crisis: The Facts, Institute for Water, Environment and Health. United Nations University, ISBN: 978-92-808-6083-2.

[2] Neena, D., Kondamareddy, K. K., Bin, H., Lu, D., Kumar, P., Dwivedi, R. K., Pelenovich, V.O., Zhao, X-Z., Gao, W., Fu, D., 2018.Enhanced visible light photodegradation activity of RhB/MB from aqueous solution using nanosized novel Fe-Cd co-modified ZnO. Scientific Reports,8, 91-106.

[3] Viswanathan, B. 2018.Photocatalytic Degradation of Dyes: An Overview.Current Catalysis, 7, 1-25.

[4] Mousavi, M., Habibi-Yangjeh, A., Pouran, S.,R., 2018. Review on magnetically separable graphitic carbon nitride-based nanocomposites as promising visible-light-driven photocatalysts. J. Mater. Sci. Mater. Electron, 29 , 1719–1747.

[5] Khalilabad, H., D., Yangjeh, A., H., Seifzadeh, D., Khaneghah, S., A., Kermani, E., V., 2019.g-C_3N_4 nanosheets decorated with carbon dots and CdS nanoparticles: Novel nanocomposites with excellent nitrogen photofixation ability under simulated solar irradiation. Ceram. Int, 45, 2542–2555.

[6] Gade, R., Ahemed, J., Yanapu, K., L., Abate, S. ,Y., Tao, Y.,T., Pola, S., 2018. Photodegradation of organic dyes and industrial wastewater in the presence of layer-type perovskite materials under visible light irradiation. JECE, 6, 4504-4513.

[7] Lin, K.,Y., A., Lin, T.,Y., 2018. Degradation of Acid Azo Dyes Using Oxone Activated by Cobalt Titanate Perovskite. Water, Air, & Soil Pollution, 51(15)1 -14.

[8] Mohanty,L., Dash,S.K.,2020. Adsorptive Removal Of MB Dye By Graphitic-C_3N_4From Industrial Effluents.IJSTR, 9, 34-2029.

[9] Ali,S., Humayun,M., Pi,W., 2020. Fabrication of $BiFeO_3$-g-C_3N_4-WO3 Z-scheme heterojunction as highly efficient visible-light photocatalyst for water reduction and 2,4-dichlorophenol degradation: Insight mechanism. Journal of Hazardous Materials,397, 122-708.

[10] Liu,Z., Ma,Z., 2020. Promoting the photocatalytic activity of $Bi_4Ti_3O_{12}$ microspheres by incorporating iron.RSC Adv, 10, 32-192.

[11] Di,L., Yang, H., Xian, T., Chen X., 2018. Enhanced Photocatalytic Degradation Activity of $BiFeO_3$ Microspheres by Decoration with g-C_3N_4 Nanoparticles.Materials Research, 21(5),1-10.

[12] Yao,w.,F., Xu,X.,H., Wang,H., 2004. Photocatalytic property of perovskite bismuth titanate.Applied Catalysis B: Environmental, 52, 109–116.

[13] Yang,B.,H., Qiang, T.,G., Yan,M.,H., Ao,X., 2010. Co-precipitation Synthesis of BiFeO3 Powders.Advanced Materials Research, 105, 286-288.

[14]Fan,T.,Chen,C.,Tang,Z.,2015.MaterialsScienceinSemiconductorProcessing,40,439–445.

[15] Khodadoost,S., Had,A., Sabet,J.,K., 2017. Journal of Environmental Chemical Engineering 5 , 5369–5380.

[16] Wang,X., Mao,W., Zhang, J., 2015. Journal of Colloid and Interface Science 448, 17–23.

[17] Meenakshi,P., Selvaraj,M., 2018. Bismuth titanate as an infrared reflective pigment for cool roof coating,.Solar Energy Materials and Solar Cells, 174, 530–537.

[18]Ke,H., Wang,W.,Wang,Y.,Xu,J., Jia,D., Lu,Z., Zhou,Y.,2011. Factors controlling pure-phase multiferroic $BiFeO_3$ powders synthesized bychemical co-precipitation. Journal. of Alloys and Compounds,509 ,2192–2197.

[19]Siddique,M.,Khan,N.M., Saeed,M., 2018. Photocatalytic Activity of Bismuth FerriteNanoparticles Synthesized via Sol-Gel Route. Z. Phys. Chem,10,1-13.

[20]Fan,T., Chen,C., Tang,Z., Ni,Y., Lu,C.,2015. Synthesis andcharacterizationofg-C_3N_4/$BiFeO_3$ compositeswithan enhanced visiblelightphotocatalyticactivity. Materials Science in Semiconductor Processing,40**,**439-445**.**

[21]Ghasemi,A., Safizade,B.,2018. Enhanced Photocatalytic Activity of Two-Pot-Synthesized $BiFeO_3$–$ZnFe_2O_4$ Heterojunction Nanocomposite. Journal of electronic materials.47,2225-2229.

[22] Lijing, Di., Yang,H., Xian,T., Chen,X., 2018. Enhanced Photocatalytic Degradation Activity of $BiFeO_3$ Microspheres by Decoration with g-C_3N_4 Nanoparticles.
Materials Research, 21(5),1-10.